

Evaluation of the Impact of Potential Fire Scenarios on Structural Elements of a Cable-Stayed Bridge

IAN BENNETTS

Noel Arnold and Associates, Melbourne, Australia

KHALID MOINUDDIN*

*Centre for Environmental Safety and Risk Engineering
Victoria University, P.O. Box 14428, Melbourne
Victoria 8001, Australia*

ABSTRACT: It has become necessary to consider the potential exposure of major bridges to flames from oil or liquefied petroleum gas fires as part of comprehensive risk assessments being undertaken for major infrastructure. This article identifies and characterizes potential fire scenarios relevant for bridges and considers the likely impact on elements of a bridge structure. As part of this study, simplified heat transfer models are developed for the purpose of determining the temperatures of key structural steel elements. These models, which provide an efficient method for determining heat transfer through elements such as heavy bundled steel cable, are described in this article. The Newton–Raphson method is used to solve the key equations. Calculated temperatures are presented for the various fire scenarios involving key structural steel elements and the implication of these temperatures for the structural behavior of the steel elements is considered.

KEY WORDS: cable-stayed bridge, steel cable, heat transfer, bridge fire scenario.

INTRODUCTION

BRIDGES ARE DESIGNED to resist a range of applied loads such as wind, earthquakes, self-weight, and live loading including the variable loading associated with traffic. The possibility of fire and its effect on a bridge structure should also be considered by the design engineer. A fire associated with a bridge will most likely be the result of a vehicle fire associated

*Author to whom correspondence should be addressed. E-mail: Khalid.Moinuddin@vu.edu.au

with a truck, bus, or train, depending on the traffic on and below the bridge. An engineering approach, as opposed to a regulatory approach, should be used to determine the range of possible fire scenarios and the likely consequences for a bridge structure.

Modern bridges that span normal roadways are typically designed such that the bridge girders between piers resist the imposed loads through beam action. Long-span bridges are necessary where regular piers cannot be provided due to the clear spaces that must be maintained across land or sea. Such long spans can best be achieved through a combination of the flexural resistance of the girders and a vertical supporting system utilizing cables located above the bridge deck. Some of the renowned cable-stayed bridges are Tataru Bridge in Japan, Clark Bridge (Alton, Illinois), Maumee Bridge (Ohio), and Sunshine Skyway bridge (Tampa, Florida) in the USA, Vancouver Skybridge in Canada, The Normandy Bridge in France, Rama VIII Bridge in Thailand, to name a few. In Australia, two such bridges are the Westgate Bridge in Melbourne and Eleanor Schonell Bridge in Queensland. Pictures of two famous cable-stayed bridges are shown in Figure 1, where cables are used to provide vertical support to the girders located below the bridge deck. It can be observed that the critical supporting elements are located below the deck of the bridge. This is again illustrated in Figure 2.

Unlike a normal short-span bridge where the potential impact of fire is rarely considered, it may be necessary to consider the impact of fire on a major cable-stayed bridge for the following reasons:

1. loss or closure of the bridge for a significant time may lead to unacceptable commercial consequences,
2. it may be impossible to undertake repairs if significant damage occurs.

This article considers fire-safety aspects of the structure represented by the generic cable-stayed bridge illustrated in Figure 2. In the event of a fire on



Eleanor Schonell Bridge, Australia



Tataru Bridge, Japan

Figure 1. Cable-stayed bridges. (The color version of this figure is available online.)

the bridge deck the girders will not be affected as the heating source is above the girders and the deck will provide adequate shielding [Figure 2 situation (a)]. However, a fire on a roadway below the deck could have a significant effect on the girders above [Figure 2 situation (b)] with the temperature reached by the girders being a function of:

1. the height of the girders above the roadway,
2. the heat release rate (HRR) and duration of the fire below the bridge span.

However, long-span bridges are usually located well above potential fire sources passing below the bridge. Furthermore, it is unusual to consider the effect of a fire under a normal road bridge on the supports for the following reasons:

1. due to the mass of the girders, it would take a significant time for girders to deform or be damaged and by this time traffic flow below the bridge will most likely have stopped, and
2. the repair of damaged girders can readily be achieved.

Therefore, fire sources under bridges are ignored in this study, which concentrates on fire sources on the bridge deck itself. Potential fire scenarios that would have the most adverse effect on structural elements are:

1. a heavy truck fire located close to the main supports or cables
2. an oil or flammable liquids tanker that catches fire when directly adjacent to the main supports or the cables. This could be the result of rupturing of the tanker following a collision with another vehicle or part of the bridge
3. a gas jet fire resulting from pipe fracture and ignition of fuel from a liquefied petroleum gas (LPG) tanker, most likely following a collision.

Steel bridge decks are usually protected with a layer of concrete and/or bitumen. It is known that bitumen is quite porous and will absorb significant

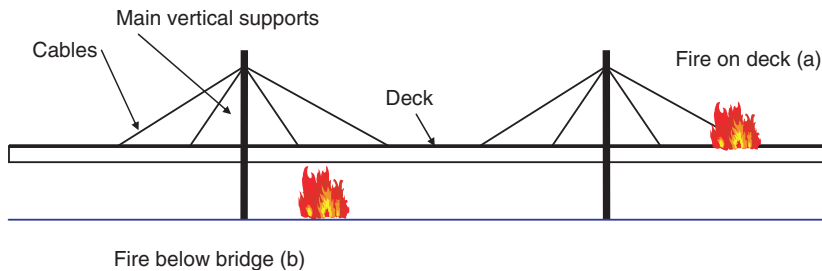


Figure 2. Generic cable-stayed bridge with fires above and below bridge deck. (The color version of this figure is available online.)

quantities of fuel, if flammable liquid spills on it. Since oxygen is needed for combustion, burning will take place at the surface of the deck. The insulating characteristics of the fuel-logged bitumen will continue to provide protection to the deck and it is not expected that significant deck temperatures will be achieved.

The main elements of the cable-stayed bridge structure that could be adversely affected by a fire are the cables and the main vertical supports. As steel is extremely strong but very flexible, steel cables are used for this type of bridge. Such cables are very economical as they allow a slender and lighter structure which is still able to span great distances. In some bridges, steel cables are protected with insulation materials such as mineral fiber blanket for fire protection and/or sheathed with stainless steel sheeting to guard against corrosion. Main vertical supports can be either reinforced concrete, composite or steel construction. This article considers steel construction.

BRIDGE STRUCTURE

In the case of a major cable-stayed bridge, the ‘stay cables’ are likely to consist of bundles of cables as illustrated in Figure 3. Each cable of the bundle is composed of multiple-wire strands often placed in a steel sheathing. The number of such cables in each ‘stay cable’ varies from bridge to bridge. Usually a set of cables are surrounded by other sets of cables forming a ring and this ring may be further surrounded by another ring and such surrounding process may continue for a number of times.

For the purpose of this study, it is assumed that there are 4 (76 mm diameter) inner cables surrounded by 12 (73 mm diameter) outer cables (as shown in Figure 3(a)). The situations associated with both insulated and uninsulated bundles of cables are considered. For the insulated case (as shown in Figure 3(b)), a 13 mm thick mineral fiber blanket is assumed to

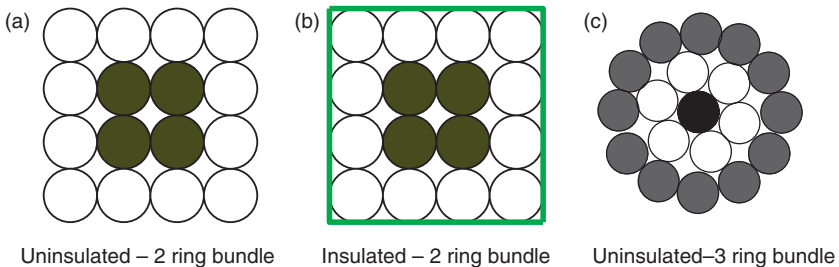


Figure 3. Cross-section of ‘Stay Cables’: (a) uninsulated – 2 ring bundle, (b) insulated – 2 ring bundle, (c) uninsulated–3 ring bundle. (The color version of this figure is available online.)

encapsulate the complete bundle of cables and for the mineral fiber to be encapsulated with 3 mm thick stainless steel sheeting to give adequate protection from the weather.

For the purpose of this article only, the vertical cable supports are considered to have no direct thermal fire protection. The supports are box structures fabricated from heavy steel plates and can only be exposed to fire from the outside. The combined thickness is taken as 62.5 mm.

FIRE SCENARIOS

The range of fire severities (HRR and duration of burning) associated with recorded truck fires is difficult to obtain from statistical records. It is also not known with respect to the severity of fires whether the fires occurred when the trucks were stationary or moving. Most fires appear to originate within the cabin or engine compartment. For a fire to pose a danger, the fire would need to involve most of the fuel associated with the truck and for the truck to be stationary. Thus, the fire would need to cause the truck to stop and then spread to the rest of the combustibles or the fire could be the result of an accident.

It is known that 2% of heavy vehicles utilizing major traffic routes such as major bridges are flammable liquid tankers and 1% LPG tankers [1]. In the case of these tankers, particular safety and operational features are incorporated to guard against fire initiation or to mitigate the effects of a developing fire. It seems that the most critical scenario would be a collision that causes the tanker to roll over or impact heavily against one of the main supports.

In the case of an LPG tanker, the most severe fire scenario is a high-pressure gas jet resulting from fracture of a pipe on the tanker. However, this would only be a potential problem for the structure if the gas jet impinged directly on one of the key elements.

The characteristics of potential truck fires are considered in the following section.

Large Truck Fire

The length of a semi-trailer is taken as 20 m with the maximum height above ground as 4.6 m. If the trailer is involved in burning the flame height will be more a function of the width of the tray and the HRR. From empirical correlations, the resulting flame height is likely to be around 12–15 m above the tray should the truck be burning whilst upright, with the ratio of the height of flame to the truck width equal to 4–5. These estimates of flames height are based on considering HRR values of between 20 and 50 MW. However, temperatures are reduced close to the top of the flame,

with the highest temperatures closer to the base. Flame temperatures of around 800–1000°C and uniform over a lesser radiating area would be expected. If the fire is directly adjacent to the cables or vertical supports and there is no wind or the flames are being blown away from the supports or cables, then it is reasonable to model this fire as a radiant heat panel having a flame temperature of 900°C with dimensions of 20 m width by 12 m high.

The presence of wind can be significant at the top of a bridge and should be taken into account as far as its effect on flame deflection is concerned. Should the wind be blowing towards the main supports or cables, then these may be engulfed in fire and subject to both radiant and convective heating. Gusting effects associated with the wind may increase the variability of the heating effects associated with the flames. Nevertheless, the heating effect due to wind-bent flames is considered to be steady state. This heating situation is referenced as LT, and the resulting steel temperatures will be determined using transient heat flow analysis.

For this fire scenario, the resultant emissivity of flames and steel is taken as 0.62 [2] and the convective heat transfer coefficient is taken as that recommended for modeling a standard fire test exposure, i.e., 23.2 W/(m² K). As the scenario without wind will result in a less severe thermal situation, its analysis is excluded here.

Tanker Fire

The explosion of a tanker with the sudden release of heat energy will not have as detrimental effect (as far as heating of the structure is concerned) as an associated pool fire caused by the leakage of fuel on to the roadway. This is due to the fact that in the case of an explosive fireball, the heat is released so quickly that very high temperatures are only experienced for a very short time.

The details of the roadway and curbs can be important with respect to the resulting flammable liquids fire. For example, if the roadway has significant slope and if there are no curbs then this will prevent containment of the fuel. The lack of containment will reduce the duration of burning but may result in greater flame height and burning over a larger area. For the purpose of this study, an unconfined fuel spill equal in diameter to a roadway of width 15 m has been adopted. Based on this pool diameter, the incident heat flux at an external target (i.e., a cable or main support) can be determined using the Shokri and Beyler correlation [3] given by:

$$\dot{q}'' = EF_{12} \quad (1)$$

where, $E = 58 \times 10^{-0.00823D}$

Here, E is the emissive power of the pool fire flame in kW/m^2 , and F_{12} is the view or configuration factor between the target and the flame. Based on a 15 m pool diameter, E is calculated as 45 kW/m^2 . However, a safety factor of 2 is suggested by the SFPE handbook [4] due to uncertainties associated with this correlation and a heat flux of 90 kW/m^2 is therefore adopted. The effective configuration factors for the steel cable are taken as 0.5 and 0.66 for unprotected and insulated cases, respectively [5]. These configuration factors take account of the fact that individual cables at the sides and rear of the bundle do not see as much of the radiation heat flux as those at the front of the bundle. For the main support only the exposed face of the support is considered and F_{12} is taken as unity.

The effects of wind blowing in the direction of the cables and main supports have been determined using empirical correlations. For winds of greater than 2 m/s the flames may impinge directly on the cables or the main support structure up to a height above the roadway of 25 m. In the worst-case scenario, the structural elements are considered to be within the pool and will be heated by both radiation and convection. Experimentally measured heat fluxes of up to 170 kW/m^2 have been measured within the pool [4].

A pool fire centered on roadway with the presence of wind such that the flames are blown against the supports or cables is denoted as TF. A fire situation in the absence of wind is excluded, as this poses a less severe thermal condition.

LPG Tanker Fire

An LPG explosion with a sudden release of energy is a possibility. This would start from a sudden release of gas from the tank and ignition of the resulting vapor cloud. A fireball of diameter 100–150 m (assuming a tanker with 30,000 kg of gas) could be formed [4]. The associated emissive power of the fireball may be up to 350 kW/m^2 for a few seconds. However, since the potential exposure of the structure is very short, little heating of the structure will take place.

Fracture of a pipe leading to the emission of high-velocity gases in any direction may result in localized heating of cables or main support structure. It is also possible that the gases under pressure may not ignite or that the gas jet may miss the structural elements altogether. Clearly, this is a very unlikely scenario. Tests on 50 mm diameter pipes releasing 8 kg/s of gas at 13 bar (i.e., 1.3 MPa) pressure have been conducted. Flame lengths of up to 35 m were obtained with gas temperatures of 1300°C at 4 m and 1200°C at 25 m from the source. The latter corresponds to a total heat flux of 250 kW/m^2 [4].

This fire is denoted as LPG fire and is taken as direct impingement of high-velocity flames to give a total heat flux of 250 kW/m^2 . The presence of high-velocity flames presents potentially an erosion problem for cladding materials (fire protective or corrosion resisting). The protection of such materials by a suitable means of encapsulation (e.g., stainless steel sheeting) will be necessary.

For all fire scenarios, the duration has been taken as 2 hours. However, the actual duration will be dictated by the quantity of fuel and the rate at which it is being consumed.

ESTIMATED TEMPERATURE OF STRUCTURAL ELEMENTS

The effect of the above fires on the cables and main support structure is now considered. This is done using several transient heat flow models. The protected and unprotected cables and the unprotected main support structure are analyzed.

Thermal Analysis of Protected Cables

This has been done by reasonably assuming that the combination of the outermost cables act as a lumped mass [gray cables in Figure 3(c)]. The immediately inner cables [six white cables in Figure 3(c)] are also treated as a lumped mass and receive heat from the 12 outer gray cables by radiation only, since the contact area between the two sets of cables is very small. Similarly the innermost cables [one black cable in Figure 3(c) and four black cables in Figure 3(a) and 3(b)] are also treated as a lumped mass and receive heat from immediately outer ring of cables [six white cables in Figure 3(c) and 12 white cables in Figure 3(a) and 3(b)] by radiation only. The same process is assumed between the successive rings at intermediate positions.

For protected cables, the insulation material is usually placed surrounding the outermost steel cables and encapsulated by a steel sheet. It is expected that in the event of a fire, the temperature of that sheet will be very close to the temperature of the outer face of the insulation. The problem is solved by two modeling approaches:

1. The first model assumes that an air gap exists between the insulation and the outermost cables [Figure 3(b)]. In this case, heat is first radiated from the flame to the steel sheet, then conducted through the insulation, then radiated from the inside surface of the insulation to the outermost cables and then radiated to the innermost cables.

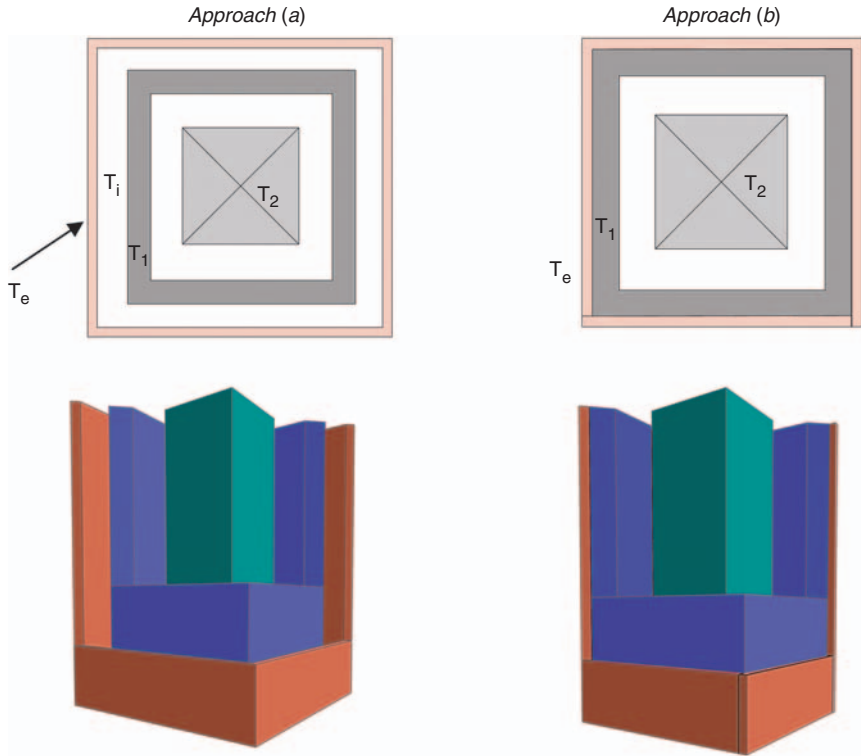


Figure 4. Transient heat flow model: (top) plan view and (bottom) cut away 3D view. (The color version of this figure is available online.)

- In the case of the second model, the insulation is assumed to be in direct contact with the outermost cables. Heat is first radiated from the flame to the steel sheet, then conducted through the insulation to the outer cables and then radiated from the outermost cables to the innermost cables.

The true situation is expected to be somewhere between (a) and (b). Figure 4 illustrates these approaches for the cable arrangement shown in Figure 3(b). In these figures, the outermost square hollow duct represents the 13 mm thick insulation, the middle square hollow section represents the lumped mass of the 12 outer cables and the center square column represents the lumped mass of the four inner cables. For the analysis, a unit length of cable is considered.

The equations corresponding to the two models are now constructed. The fire temperature is denoted as T_f , while the temperatures of the outer and

inner faces of the insulator are represented by T_e and T_i , respectively. On the other hand, the temperatures of lumped mass 1 through to n are denoted as T_1, T_2, \dots, T_{n-1} and T_n , respectively. Note that for Figure 4, $n=2$ and for case (b) $T_i = T_1$.

Transient Heat Flow Model for Approach (a)

The above geometry/model has $n+2$ unknown temperatures. To carry out the analysis, the following $n+2$ equations are constructed based on conservation of energy.

Equation 1: Heat enters (transferred) from the fire via convection and radiation to the control volume 1 (Figure 5), no heat is stored and heat leaves the control volume via conduction through the insulation layer. Conduction through the insulation layer is assumed linear.

$$\underbrace{F\alpha(T_f - T_e)}_{\text{convection}} + \underbrace{\sigma\varepsilon F_{12}(T_f^4 - T_e^4)}_{\text{radiation}} = \frac{k}{d}(T_e - T_i)$$

Here,

k = thermal conductivity of the insulator, mineral insulation blanket, 0.5 W/(m K)

d = insulator thickness, 13 mm

ε = emissivity

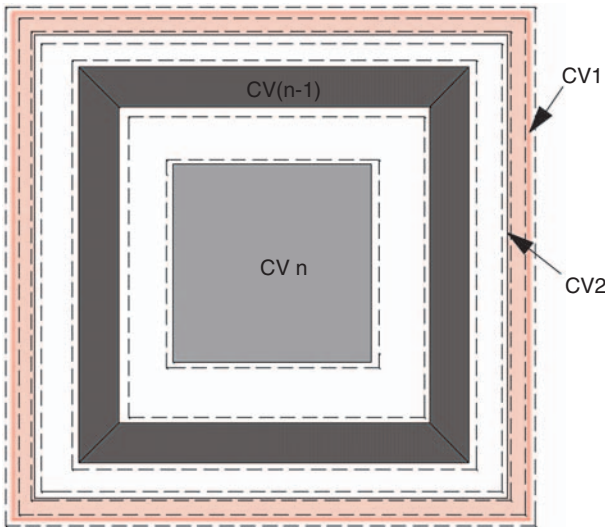


Figure 5. Control volume for approach (a), CV represents control volume. (The color version of this figure is available online.)

α = convective heat transfer coefficient, 23.2 W/(m² K)

σ = Stefan-Boltzmann constant, [W/(m² K⁴)]

F = convection factor, usually 1. If there is no convective heating then F is zero

F_{12} = configuration factor. If the structural elements are engulfed in fire then F_{12} is unity. For protected and unprotected cables its values are 0.5 and 0.66, respectively, while the cables are not engulfed using the approximate approach by Law and O'Brien [5].

Equation 2: Heat enters the control volume 2 (Figure 5) via conduction through the insulation layer, no heat is stored and heat leaves the control volume via radiation from the inner face of the insulator to the outer face of the lumped mass 1.

$$\frac{k}{d}(T_e - T_i) = \sigma\varepsilon(T_i^4 - T_1^4)$$

Equation 3: Energy (heat) balance for the lumped mass 1 (control volume $n - 1$ in Figure 5) is taken as the heat absorbed by the lumped mass 1 being equal to the difference between the heat radiated from the inner face of the insulator to the outer face the lumped mass 1 and the heat radiated from the inner face of the lumped mass 1 to the outer face of lumped mass 2. That is,

$$A_1\sigma\varepsilon(T_i^4 - T_1^4) = A_2\sigma(T_1^4 - T_2^4) + c_{s1}\rho V_1 \frac{\Delta T_1}{\Delta t}$$

Here,

t = time

c_{s1} = specific heat capacity of the lumped mass 1 of steel [kJ/t/K],

$$3.8 \times 10^{-4} T_1^2 + 2 \times 10^{-1} T_1 + 472$$

ρ = steel density taken as 6.68 t/m³

V_1 = volume of the lumped mass 1

$A_1 = A_{1_out}$ (Table 1)

$A_2 = \frac{A_{2_out} A_{1_in} \varepsilon}{A_{2_out} + A_{1_in} - A_{1_in} \varepsilon}$ (taken from Heat Transfer by Holman [6])

Table 1. Dimension of lumped masses.

Square ring no	Outer surface area per m of length, A_{out} , (m ²)	Inner surface area per m of length, A_{in} , (m ²)	Volume per unit length (m ³)
1	1.168	0.748	0.05
$n(=2)$	0.54	-	0.018

This equation will be repeated based on the number of rings that exist for the bridge cable. If there are n rings, then there will be $(n - 1)$ similar equations.

Equation $n + 2$: Energy (heat) balance for the last (n -th) lumped mass (located at the center represented as control volume n in Figure 5) is taken as the heat absorbed by the n -th lumped mass being equal to the heat radiated from the inner face of the $(n-1)$ -th lumped mass to the outer face of the n -th lumped mass. That is,

$$A_n \sigma \varepsilon (T_{n-1}^4 - T_n^4) = c_{sn} \rho V_n \frac{\Delta T_n}{\Delta t}$$

Here,

c_{sn} = specific heat capacity of the lumped mass n of steel [kJ/t/K],

$$3.8 \times 10^{-4} T_n^2 + 2 \times 10^{-1} T_n + 472$$

V_n = volume of the lumped mass n

Transient Heat Flow Model for Approach (b)

This model has $n + 1$ unknown temperatures, as $T_i = T_1$. To carry out the analysis, the following $n + 1$ equations are constructed again based on conservation of energy.

Equation 1: Heat enters (transferred) from the fire via convection and radiation to the control volume, no heat is stored and heat leaves the control volume via conduction through the insulation layer. Conduction through the insulation layer is assumed linear.

$$\underbrace{F\alpha(T_f - T_e)}_{\text{convection}} + \underbrace{\sigma \varepsilon F_{12}(T_f^4 - T_e^4)}_{\text{radiation}} = \frac{k}{d}(T_e - T_1)$$

Equation 2: Energy (heat balance) for the lumped mass 1 is taken as the heat absorbed by the lumped mass 1 being equal to the difference between the heat enters from the inner face of the insulator to the outer face the lumped mass 1 via conduction and the heat radiated from the inner face of the lumped mass 1 to the outer face of lumped mass 2. That is,

$$A_1 \frac{k}{d}(T_e - T_1) = A_2 \sigma (T_1^4 - T_2^4) + c_{s1} \rho V_1 \frac{\Delta T_1}{\Delta t}$$

Equation 3: Energy (heat balance) for the lumped mass 2 is taken as the heat absorbed by the lumped mass 2 being equal to the difference between the heat radiated from the inner face of the insulator to the outer face the

lumped mass 2 and the heat radiated from the inner face of the lumped mass 2 to the outer face of lumped mass 3. That is,

$$A_2\sigma\varepsilon(T_1^4 - T_2^4) = A_3\sigma(T_2^4 - T_3^4) + c_{s2}\rho V_2 \frac{\Delta T_2}{\Delta t}$$

This equation will be repeated based on the number of rings exists for the bridge cable. If there are n rings, then there will be $(n - 2)$ equations.

Equation $n + 1$: Energy (heat) balance for the last (n -th) lumped mass (located at the center) is taken as the heat absorbed by the n th lumped mass being equal to the heat radiated from the inner face of the $(n - 1)$ -th lumped mass to the outer face of the n -th lumped mass. That is,

$$A_n\sigma\varepsilon(T_{n-1}^4 - T_n^4) = c_{sn}\rho V_n \frac{\Delta T_n}{\Delta t}$$

Results of Analysis

In this study, temperature analysis is done only for the protected cable arrangement shown in Figure 3(b). The properties adopted for the cables are summarized in Table 1. Here, ring 1 represents the outermost ring and ring n represents the innermost lumped mass.

As there were only two rings of cables, for approach (a) four equations have been solved and for approach (b) three equations have been solved ignoring Equation 3. In each case, the equations have been solved by the Newton–Raphson iteration method using a forward finite difference approach. After conducting a time-step sensitivity analysis, a time-step of 15 seconds was adopted.

The cable temperatures are likely to be somewhere between the predictions given by (a) and (b). The calculated cable temperatures using Approaches (a) and (b) are given in Figure 6.

It can be seen in Figure 6 that for approach (b), the increase in temperature is greater. There is a significant advantage in maintaining an air gap between the insulation and the outer face of the outer cables.

Thermal Analysis of Unprotected Cable

For the unprotected cable, the insulation layer is removed as shown in Figure 7 such that the outside of the cable is directly exposed to fire.

Transient Heat Flow Model

The above geometry/model involves n unknown temperatures. To solve these temperatures n equations are required.

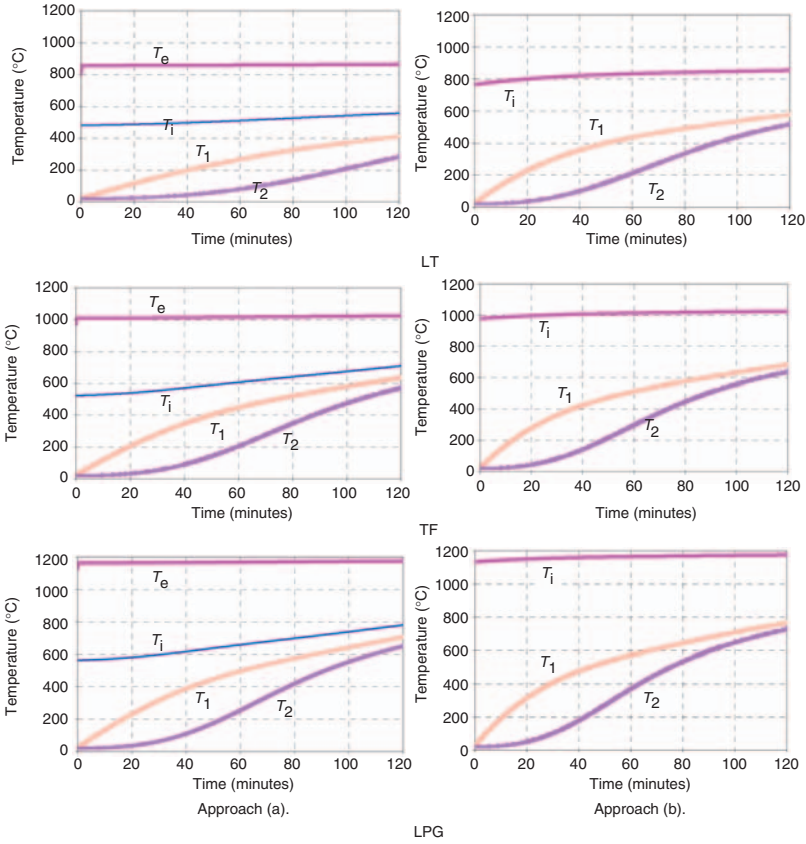


Figure 6. Results of protected cable analysis. (The color version of this figure is available online.)

Equation 1: Heat transferred from fire to lumped mass 1 is equal to the heat absorbed by lumped mass 1 plus that radiated to lumped mass 2.

$$\underbrace{F\alpha(T_f - T_1)}_{\text{convection}} + \underbrace{\sigma\epsilon F_{12}(T_f^4 - T_1^4)}_{\text{radiation}} = c_{s1}\rho V_1 \frac{\Delta T_1}{\Delta t} + A_2\sigma\epsilon(T_1^4 - T_2^4)$$

Equation 2: Energy (heat balance) for the lumped mass 2 is taken as the heat absorbed by the lumped mass 2 being equal to the difference between the heat radiated from the inner face of the insulator to the outer face the lumped mass 2 and the heat radiated from the inner face of the lumped mass 2 to the outer face of lumped mass 3. That is,

$$A_2\sigma\epsilon(T_1^4 - T_2^4) = A_3\sigma(T_2^4 - T_3^4) + c_{s2}\rho V_2 \frac{\Delta T_2}{\Delta t}$$

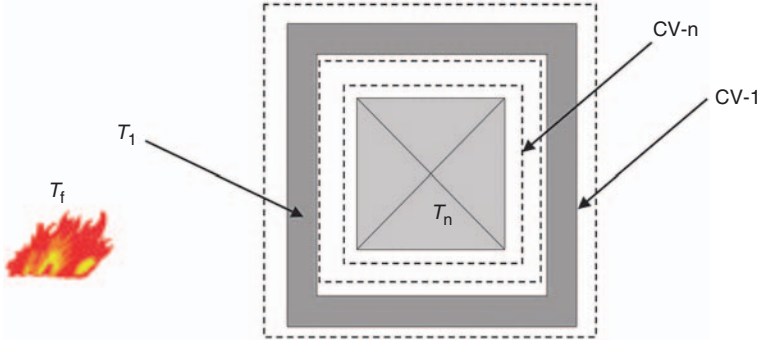


Figure 7. Transient heat flow model for the unprotected cable. (The color version of this figure is available online.)

This equation will be repeated based on the number of rings that exist for the bridge cable. If there are n rings, then there will be $(n - 2)$ equations.

Equation n : Heat transferred to lumped mass $(n - 1)$ by radiation must be absorbed by lumped mass n .

$$A_n \sigma \varepsilon (T_{n-1}^4 - T_n^4) = c_{sn} \rho V_n \frac{\Delta T_n}{\Delta t}$$

Results of Analysis

As there were only two rings of cables, two equations have been solved ignoring Equation 2 for each of the fire scenarios. The resultant temperature histories are given in Figure 8.

Thermal Analysis of Main Support Element

The main supports are welded box structures and it is unlikely, due to their size, that the entire perimeter could be heated at one time. Since this is the case, only one of the 63.5mm steel plates forming the box has been analyzed. It has been assumed that this plate is only exposed to fire on one side and that the plates forming the other sides will receive radiated heat. This situation has been modeled by considering two plates – one exposed to fire on its external face and the other parallel plate, not exposed to fire, but capable of being heated by radiation from the heated plate. No heat loss due to radiation to the surroundings for the unexposed plate has been considered. The plates are assumed to be uniformly heated. The following two equations have been solved:

$$\underbrace{F\alpha(T_f - T_1)}_{\text{convection}} + \underbrace{\sigma\varepsilon F_{12}(T_f^4 - T_1^4)}_{\text{radiation}} = c_{s1}\rho V_1 \frac{\Delta T_1}{\Delta t} + A_2\sigma\varepsilon(T_1^4 - T_2^4),$$

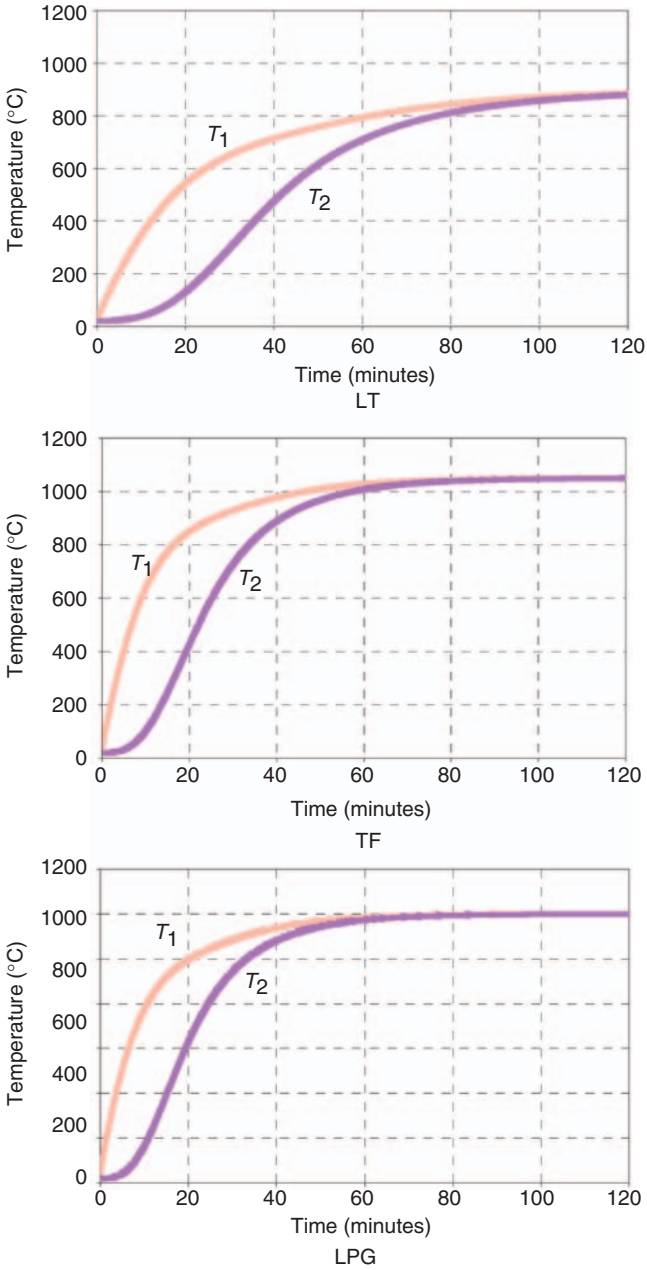


Figure 8. Results of unprotected cable analysis. (The color version of this figure is available online.)

and

$$A_n \sigma \varepsilon (T_{n-1}^4 - T_n^4) = c_{sn} \rho V_n \frac{\Delta T_n}{\Delta t}$$

The results of this analysis are given in Figure 9 for each of the fire scenarios. The temperatures of the exposed and unexposed plates (represented as T_1 and T_2) are plotted.

EFFECT OF TEMPERATURE ON MATERIAL STRENGTHS

Protected Cables

Usually the cables are made from high strength wire that has been significantly cold drawn to get the desired properties. This being the case, the relevant strength reduction versus temperature relationship is given in [7]. This was derived experimentally for high strength prestressing wire. Given the temperature of each of the bundles and the strength temperature relationship it is possible to plot the residual strength as a function of time of fire exposure for each of the fire scenarios.

Under fire conditions, the load shared by each cable is dictated by the amount of resistance that each cable is capable of carrying. The effect of increased temperature is to not only reduce strength but also increase ductility. Should some cables initially carry a greater load due to the fact that they are stiffer (stiffness is less affected by fire) and if such cables are unable to resist this load, then it will plastically deform, therefore transferring load to the other cables. In the limit, each cable resists load in proportion to its area and in proportion to the ambient temperature capacity that exists.

Since the cables are in tension, the load will be shed from the hotter outer bundle of cables (modeled as mass $n - 1$) to the inner bundle (modeled as mass n). The resultant tensile load capacity for the entire cable can therefore be determined by adding the contribution from the two bundles given the temperatures of the respective bundles. This strength is then divided by the ambient temperature strength of the entire cable. The corresponding residual strength for all three cases is plotted in Figure 10. This value gives the strength of the entire cable after a given time of fire exposure. The significant advantage in maintaining an air gap between the insulation and the outer face of the outer cables is evident in Figure 10.

Unprotected Cables and Main Support

The residual strengths for the unprotected cables have been similarly calculated and are given in Figure 11. It should be noted that the strength

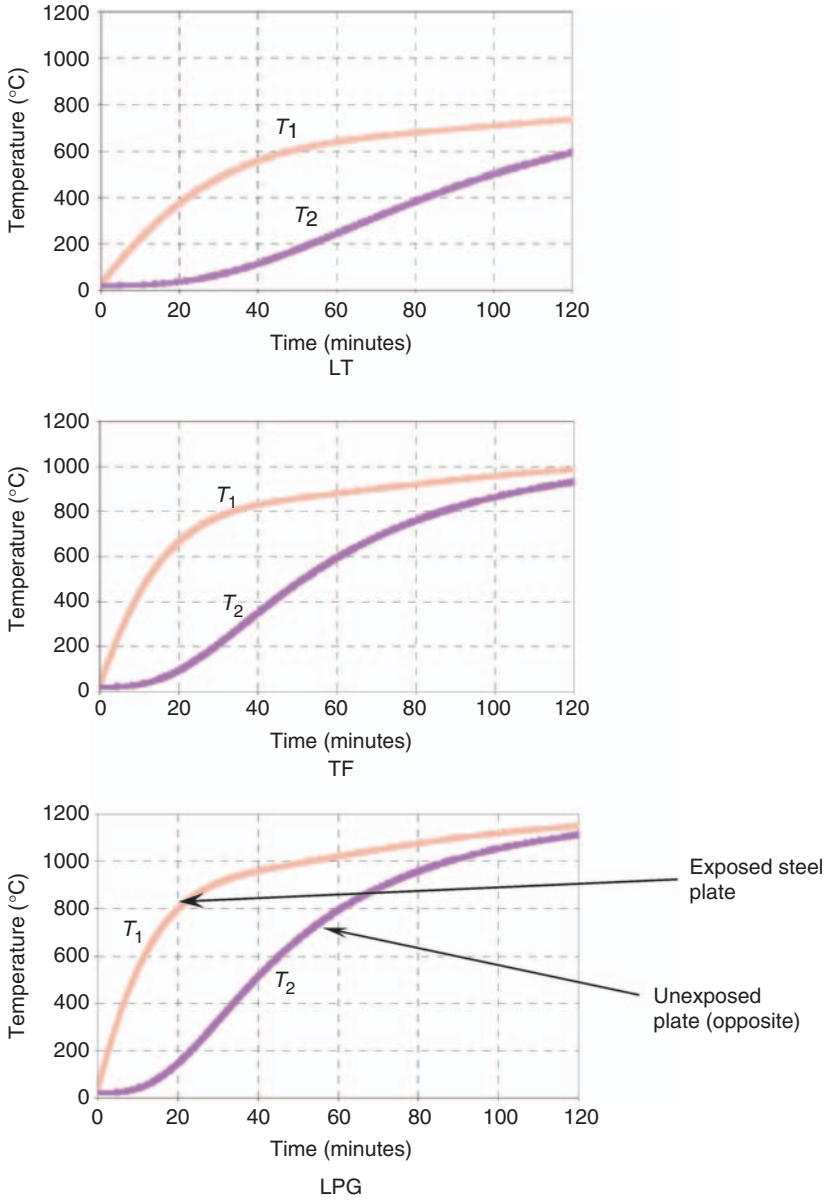


Figure 9. Results of unprotected main support analysis. (The color version of this figure is available online.)

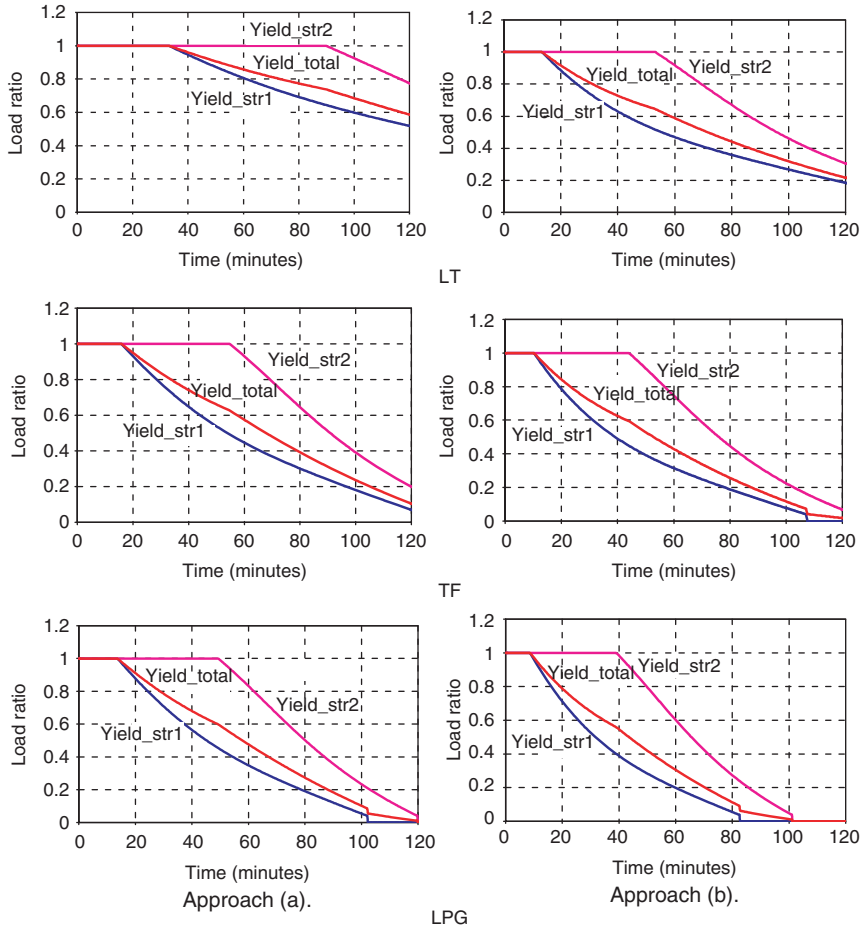


Figure 10. Temperature effects on cable strength. (The color version of this figure is available online.)

drops off much more rapidly with the time of fire exposure compared with the protected cables.

In the case of the plate associated with main support, the residual strength has been determined based on the strength versus temperature relationship given in AS4100 for structural steel [8]. The results for exposed steel plates are plotted in Figure 12 for each of the scenarios.

Summary

The results for all fire scenarios are now summarized. Tables 2 and 3 summarize the failure times for various load ratios. The information can be

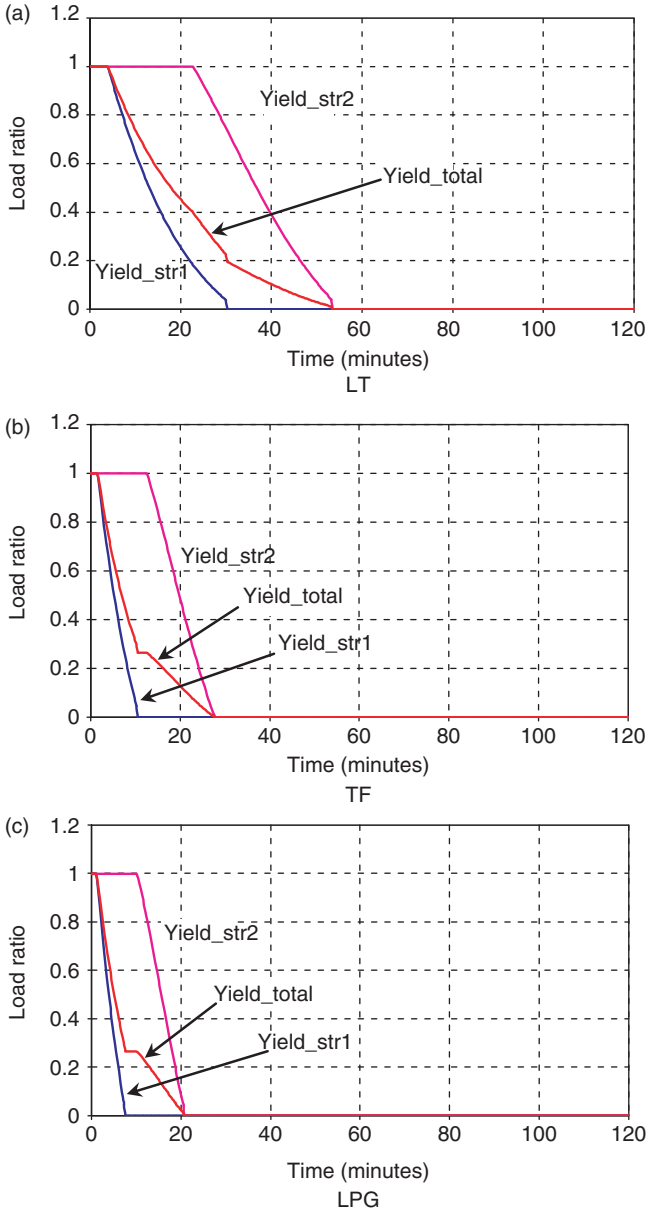


Figure 11. Temperature effects on the unprotected cable: (a) LT, (b) TF, (c) LPG. (The color version of this figure is available online.)

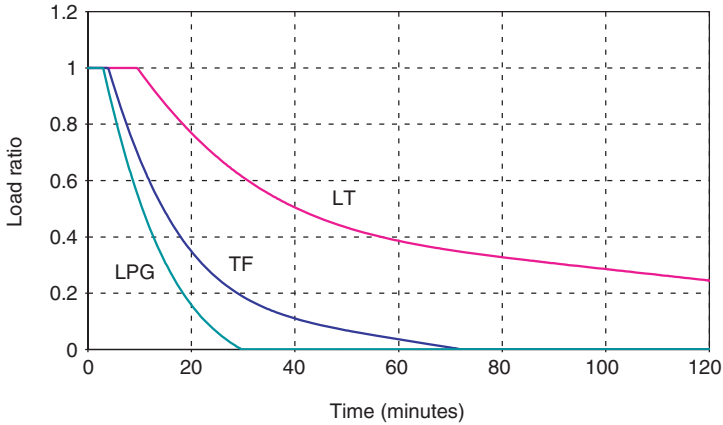


Figure 12. Temperature effects on the unprotected main support plate. (The color version of this figure is available online.)

Table 2. Time (minutes) to failure at given load ratio for protected cable.

Fire scenario	Load ratios (applied load/ultimate strength)									
	Cable (approach A)					Cable (approach B)				
	0.1	0.2	0.3	0.4	0.5	0.1	0.2	0.3	0.4	0.5
LT	>120	>120	>120	>120	>120	>120	>120	103	86	71.5
TF	>120	105	91.5	79	68	102.5	87.5	74.5	63	53
LPG	100.5	88	77	67	58	81.5	70.5	60.5	51.5	43.5

Table 3. Time (minutes) to failure at given load ratio for unprotected cable and the main support.

Fire scenario	Load ratios (applied load/ultimate strength)									
	Unprotected cable					Unprotected main support (exposed face only)				
	0.1	0.2	0.3	0.4	0.5	0.1	0.2	0.3	0.4	0.5
LT	40.5	30	26.5	22.5	17.5	>120	>120	93	56.5	40.5
TF	21.5	16.5	10	8.5	7	42	29	22.5	17.5	14.5
LPG	17	13	7.5	6	5	22.5	18.5	15	12.5	10.5

utilized as part of an engineering assessment of the potential consequences of the scenarios.

CONCLUSIONS

Calculations of the type presented in this article are an example of those that can be used to assess the vulnerability of bridge structures to the effects of fire. The analysis presented here is a simplified version, and cannot easily be extended to complex bridge structures, due to factors such as redundancy, redistribution of moments, geometric and material non-linearity, etc. Furthermore, the failure limit states adopted in the analysis based on critical steel temperature may not be applicable for complex structures.

For the particular cable situation studied, the application of a thin layer of mineral fiber insulation material, even for the most severe scenarios, will maintain structural adequacy until exhaustion of fuel or effective fire fighting can take place. On the other hand, analysis of the unprotected cable and main support plate indicates that exposure to a tanker pool fire or an LPG fire could result in high temperatures within relatively short times.

As far as the main supports are concerned, the exposed plate could lose significant strength in a short time if exposed to the more serious fire scenarios such as direct exposure to an LPG jet or exposure to the flames from a pool fire. This may not lead to failure of the main support since it is composed of other cooler plates. If these other plates are not capable of providing the necessary capacity then it may be necessary to protect the main support.

REFERENCES

1. Westgate Bridge LPG and Petrol Transportation Quantified Risk Analysis. Connell Wagner Pty Ltd and Mott MacDonald Group, June 1996.
2. Pettersson, O., Magnussen, S.E. and Thor, J., *Fire Engineering Design of Steel Structures*, Swedish Institute of Steel Construction, 1976.
3. Shokri, M. and Beyler, C.L., "Radiation from Larger Pool Fires," *Journal of Fire Protection Engineering*, Vol. 4, No. 1, 1989, pp. 141–150.
4. Beyler, C.L., *Fire Hazard Calculations for Large, Open Hydrocarbon Fires*, SFPE Handbook of Fire Protection Engineering, Chapter 3-11, 3rd edn, NFPA, Quincy, MA, USA, 2002.
5. Law, M. and O'Brien, T., *Fire Safety of Bare External Structural Steel*, Constrado, UK, 1968.
6. Holman, J.P., *Heat Transfer*, 9th edn, McGraw-Hill, New York, 2002.
7. Bennetts, I., *Further Studies on the Elevated Temperature Strength of Steel Reinforcement*, BHP Melbourne Research Lab Report, MRL/PS23/82/004, 1982.
8. Australian Standard-Steel Structures, AS4100-1998, 1998.